Acta Technica Napocensis: Civil Engineering & Architecture
Volume 66, No. 1 (2023)
Journal homepage : https://actacivil.utcluj.ro/
ISSN 234-4711, ISSN-L 1221-5848

Enhancing Seismic Performance of Precast Concrete Structures through Novel Beam-to-Column Connections

Marius G.L. Moldovan[1], Mihai Nedelcu[2]

[1,2] *Technical University of Cluj-Napoca, Faculty of Civil Engineering. 15 C Daicoviciu Str., 400020, Cluj-Napoca, Romania*

(Received 17 March 2023; Accepted 15 June 2023)

Abstract

Precast concrete structures, despite their growing popularity and numerous advantages, face challenges related to structural continuity disruption, which significantly impacts seismic design. Existing dowel connections, which should remain elastic during seismic events, often form partial failure mechanisms due to plastic deformations, thereby diminishing the assumed dissipative potential of the structure. Past research has highlighted the inefficiency of the two-dowel connection system in providing sufficient capacity for achieving column failure under cyclic loads, a key dissipative mechanism for inverted pendulum systems. Hence, there is a compelling need to improve the behaviour of beam-to-column connections in seismically active areas. This research proposes a new connection solution that offers substantial capacity improvements over the conventional dowel connection. The capacity of the proposed connection was evaluated against results derived from calibrated finite element models based previous experimental data. Furthermore, the unique configuration of the connection provides possibility for further enhancements, with individual elements adjustable to optimize efficiency. The findings support the potential of the proposed connection as a viable alternative.

Rezumat

Structurile din beton prefabricat, în ciuda popularității lor în creștere și a numeroaselor avantaje, se confruntă cu provocări legate de întreruperea continuității structurale, ceea ce afectează semnificativ proiectarea seismică. Conexiunile existente cu dornuri, care ar trebui să rămână elastice în timpul evenimentelor seismice, formează adesea mecanisme parțiale de cedare datorită deformărilor plastice, reducând astfel potențialul disipativ presupus al structurii. Cercetările anterioare au evidențiat ineficiența acestui sistem de conexiune cu două dornuri în oferirea unei capacități suficiente pentru a realiza cedarea stâlpilor sub încărcături ciclice, un mecanism disipativ cheie pentru sistemele de tip pendul inversat. Prin urmare, există o nevoie imperativă de a îmbunătăți comportamentul conexiunilor între grinzi și stâlpi în zonele cu activitate seismică. Această lucrare propune o nouă soluție de conexiune care oferă îmbunătățiri substanțiale ale capacității față de conexiunea convențională cu dornuri. Capacitatea conexiunii propuse a fost evaluată în raport cu rezultatele obținute din modele cu element finit calibrate pe baza datelor experimentale anterioare. În plus, configurația conexiunii oferă posibilitatea unor îmbunătățiri

[1] Corresponding author: E-mail address: george.moldovan@mecon.utcluj.ro
[2] Author: E-mail address: mihai.nedelcu@mecon.utcluj.ro

ulterioare, cu elemente individuale ajustabile pentru a optimiza eficiența. Rezultatele susțin potențialul conexiunii propuse ca o alternativă viabilă.

Keywords: Precast concrete structures, seismic design, dowel connections, novel connection, capacity improvements.

1. Introduction

Precast structures employ a variety of connection types, including dowel connections, wet connections (cast in situ), and emulative dry mechanical connectors [1]. Dowel connections are particularly popular in Europe, but they sometimes fail due to friction strength limitations when used in structures designed for vertical loads. In addition to friction strength issues, these connections may suffer from inadequate connector detailing, which can be attributed to a poor understanding of their behaviour and a lack of code requirements governing their use [2, 3]. As seismic risk has become a more pressing concern in recent years, the focus has shifted toward mitigating these risks and examining the effectiveness of commonly implemented solutions. The vulnerability of precast connections during seismic events has been repeatedly demonstrated in events such as the earthquakes in Emilia Romagna, Kocaely, and L'Aquila [4-9] . Researchers who conducted field studies after the Emilia Romagna earthquake reached a consensus that the failure of beam-to-column connections and unseating of the beams were two major factors contributing to the structural damage of precast systems [4, 10-12]. The seismic performance of precast structures is heavily influenced by the behaviour of the components that ensure the connection between structural elements and between these and non-structural elements [5, 11, 13].

When compared to cast-in-situ reinforced concrete structures, precast structures tend to be more vulnerable during seismic events [14]. This vulnerability is particularly pronounced in structures that were designed without taking seismic provisions into account [15-17]. A significant number of precast structures in the seismic regions of Southern Europe were constructed without proper seismic detailing for connections. Many of these structures relied on dry friction resistance joints [18]. At the time, dry-friction connections were permitted by non-seismic codes, but they ultimately led to large relative displacements and a considerably increased risk of collapse [19, 20] . In response to these concerns, code updates in seismic countries no longer allow the use of friction-based connections [21, 22].

According to Eurocode 8 [21], during the design phase, it is essential to determine the role of each structural component (resisting gravity loads, gravity and seismic, and providing connection between structural elements) and the effect of the connection on overall energy dissipation capacity. Dowel connections are considered non-dissipative and should remain in the elastic range throughout a seismic event. If plastic deformations occur, a partial failure mechanism may form, which would greatly reduce the assumed dissipative potential of the structure during the design phase. The Precast EC8 project [23] studied the seismic behaviour of precast structures with pinned connections. Although the focus of the project was on the overall behaviour and ductility of precast structures, it did not pay much attention to the seismic behaviour of individual connections. In order to fill this knowledge gap, numerous researchers have committed themselves to conducting in-depth investigations into the various aspects of beam-to-column connections. These studies have focused on different types of connections, such as pure frictional connections [5, 24, 25] and those that incorporate dowels [26-28].

The precast concrete industry is experiencing growth, largely due to the many advantages it offers. These benefits include controlled manufacturing processes (mix, placement, accelerated curing), increased quality, labour efficiency, repeatability, quick assembly, flexibility in use, speed of

erection, cost-effectiveness, eco-friendliness, and sustainability. However, the disruption of structural continuity, which is an inherent feature of precast concrete structures, poses challenges for seismic design. Continuity, redundancy, and diaphragm behaviour at the story level are fundamental requirements for seismic-resistant structures, and they need special attention when designing seismic-resistant precast buildings. The key challenge is to address these specific issues without affecting some of the mentioned advantages of precast structures. As a result, there is a need to improve beam-to-column connection behaviour in seismic areas. In response to this need, many researchers have proposed and investigated new precast connections to enhance seismic performance while maintaining the benefits of precast construction. These investigations have utilized both experimental [29-34] and numerical methods [35-38] to explore innovative connection designs and techniques.

The experimental research findings presented by M. Moldovan et al. [39] indicate that the analysed two-dowel connection system lacks adequate capacity under cyclic loads to cause column failure, which is the anticipated dissipative mechanism for inverted pendulum systems. This suggests that this solution may not be suitable for seismic regions, as the dynamic loads produced by earthquakes can impact the capacity of such connections. If the expected dissipative mechanism under lateral loads does not develop properly, it can compromise the stability of the entire structure. This could result in significant material damage and, in more severe cases, human casualties. In the context of designing a precast inverted pendulum structural system subjected to extreme lateral forces, it is imperative to augment the capacity of the beam-to-column connection. While the rudimentary dowel connection might be adequate for lower magnitudes of lateral forces, it is essential to increase the beam-to-column connection capacity. To retain the geometrical configuration of the precast components (described in [39]) and engineer the structural system to securely resist high lateral forces, potentially arising during seismic events, an alternative connection system must be adopted. As a result, this research focused on a novel connection as a potential solution. The capacity of the proposed connection was compared with the results obtained from finite element (FE) models which were calibrated based on experimental results [40].

2. Description of the proposed connection

The geometric configuration of the dowel connection (Figure 1) previously studied [39, 40] presents a significant drawback when assessing the individual capacity of the rebars employed as dowels. Their capacity is substantial when axially loaded, particularly in tension, but considerably reduced when subjected to bending moment and shear loading. The impact of shear forces becomes even more pronounced when a gap exists between precast elements in the dowel connection region. This has been demonstrated by the authors in papers [39, 40], both through experimental campaigns and finite element analysis results. Another disadvantage arises from dowel placement on top of the forks; due to the small dimensions of the fork, it can be challenging or even impossible to position the dowel to satisfy the equivalent six-diameter distance towards the edge of the concrete elements, recommended by design guidelines [1]. The objective of the proposed connection is to mitigate the aforementioned dowel connection drawbacks and to fully exploit the tension capacity of embedded dowels or similar components.

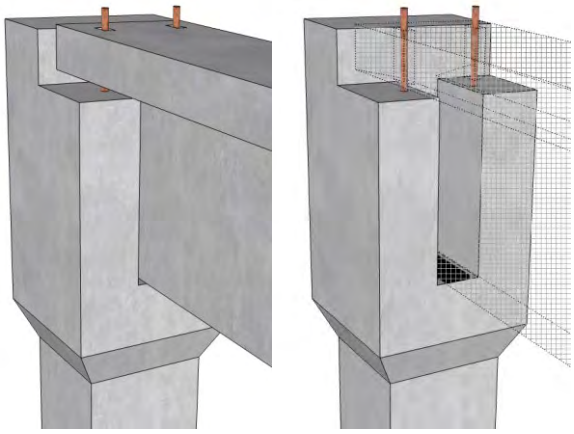

Figure 1 Beam-to-column dowel connection

In dowel connections, lateral loads are orthogonal to the connection bar; however, to enhance connection performance, they should align with both lateral loads and the precast beam. As a result, the connection bars will mainly experience axial loads. Figure 2 illustrates the proposed beam-to-column connection for an end column setup, while Figure 3 depicts a slightly altered configuration to accommodate an intermediate column supporting two beams. The connection consists of embedded bars in the column, end plates for beam attachment, securing bolts, and beam web dowel connectors (Figures 4 and 5).

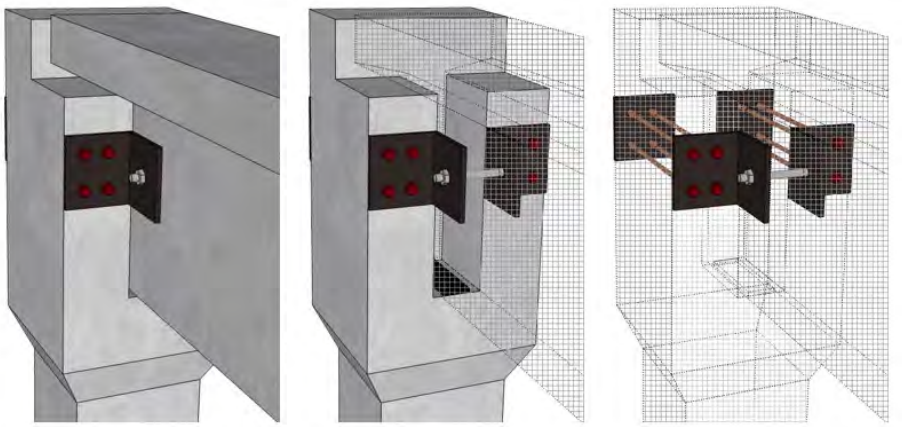

Figure 2 Connection proposal, end column perspective view

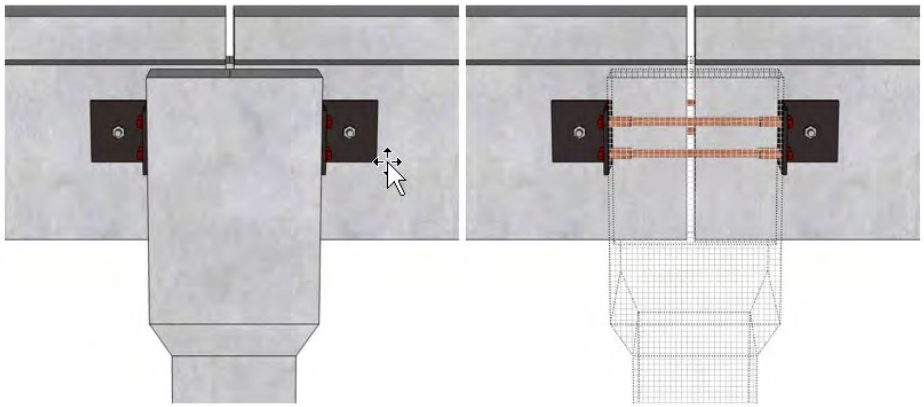

Figure 3 Connection proposal, intermediate column perspective view

Figure 4 presents the top view of the end and intermediate column connection configurations.

Embedded bars with end fittings are placed in the column before casting and are arranged parallel to the beam elements (Figure 5) to handle the axial forces from the beam. During on-site precast element assembly, end plates and L profiles are affixed to the column end using fastening bolts tightened into the end fittings of the embedded bars. The end plates prevent bar slippage under tension loads, particularly when the anchorage length is inadequate. For intermediate columns L profiles replace end plates, ensuring a symmetrical connection and supporting both beams on the column. The beam connects to the column via L profiles and a threaded dowel tightened on both sides of the beam web (Figure 4). This dowel experiences shear forces on both sides of the beam web. An advantage of this design is the diameter of the dowel can be increased to prevent shear failure. Moreover, maintaining the recommended six-diameter distance from the limits of the beam is more manageable than using dowels embedded in column forks.

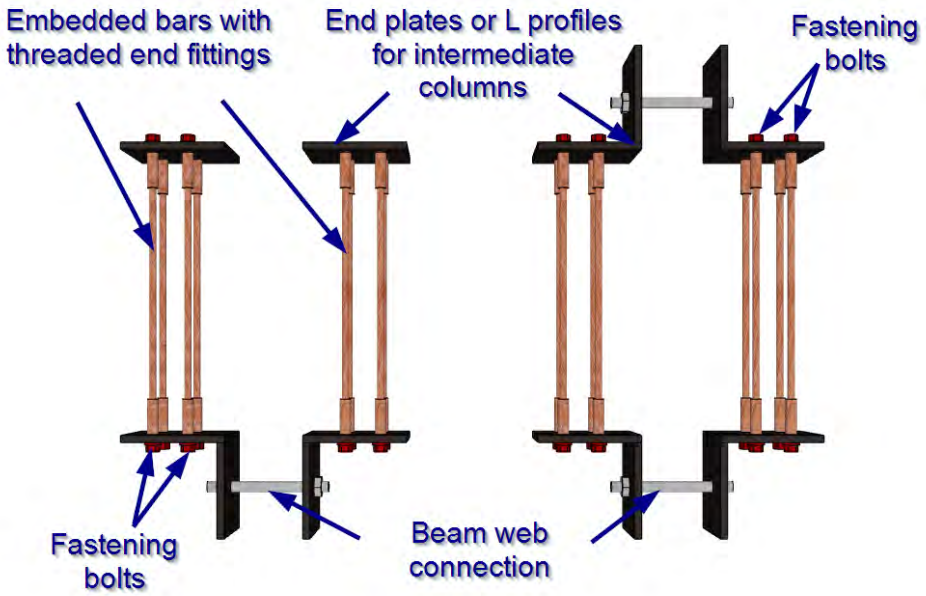

Figure 4 Assembly top view

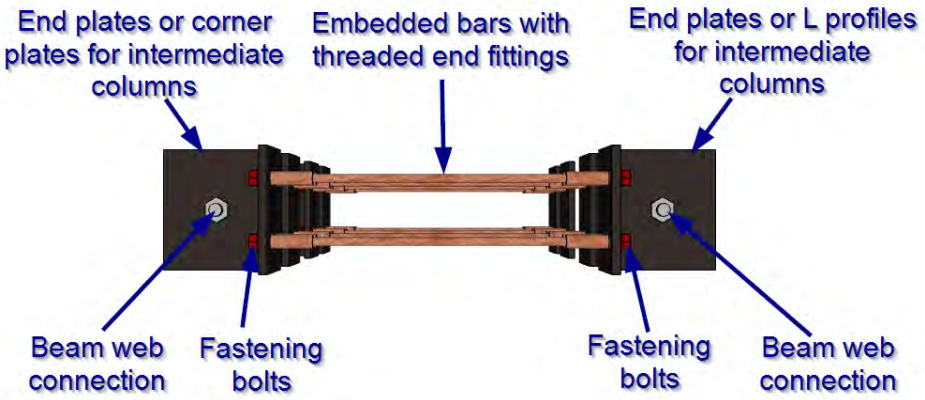

Figure 5 Assembly lateral view

The connection assembly elements can be sized according to the design force requirements, making it simpler to increase the capacity of each component compared to the previously studied dowel connection. Connection strength is also affected by the concrete capacity of precast elements, particularly the load-transmitting efficiency of the concrete and reinforcements near the beam side

of the connection. Ideally, the connection should be located at the centre of gravity of the beam cross-section to avoid unwanted effects from force eccentricity. As this proposal merely introduces the connection concept, initial assessments of individual elements should involve empirical calculations, followed by a FE analysis of the entire assembly. The capacity of the proposed connection will be compared to the capacity of the dowel connection observed in past research through experimental and finite element investigations.

3. Empirical design check of the proposed connection

The capacity of the connection is based on the weakest component. In the initial stage, component capacities are calculated using formulas provided by design codes. This section presents the geometries, dimensions, and material properties of each component in the connection assembly, which are used to compute their capacity. The longitudinal embedded bars are 25mm diameter reinforcement bars made of S500 steel with a yield strength (f_y) of 500N/mm^2 and (f_u) of 700N/mm^2 [41]. The plates and L profiles have a 20mm thickness and are made of S355 material. Figure 6 provides the dimensions for end plates and L profiles, as well as hole positions. According to EN 1993-1-1 [42], S355 steel has a yield strength (f_y) of 355N/mm^2 and an ultimate strength (f_u) of 490N/mm^2. M24 metric bolts with 8.8 material class properties were chosen for fastening. Based on EN 1993-1-8 [43], their yield strength (f_{yb}) is 640N/mm^2, and ultimate tensile strength (f_{ub}) is 800N/mm^2. An M39 metric bolt, with the same 8.8 material class as the M24 bolt, was selected for the beam connector element. Steel plate hole diameters were calculated according to bolt nominal diameter and clearance values provided in EN 1090-2 [44]. The standard specifies clearances for normal, oversized, and slotted holes. In this phase, holes are considered normal, and Table 1 shows the diameters based on bolt size.

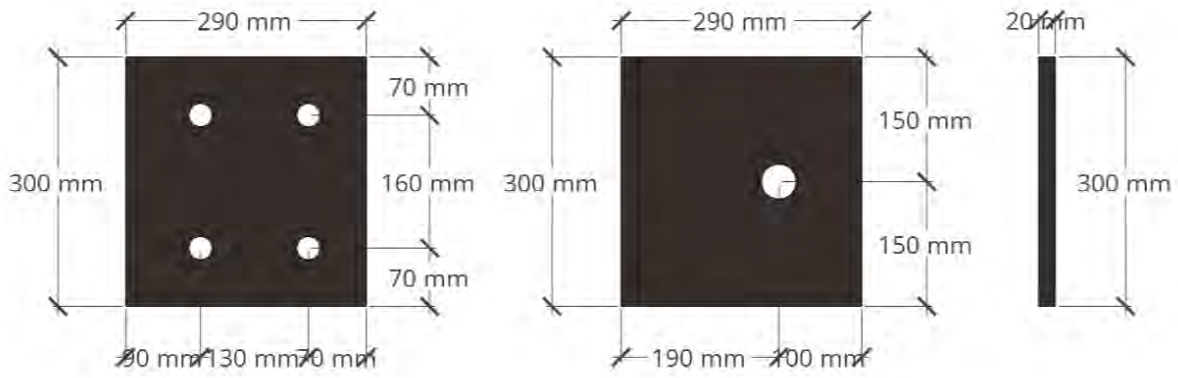

Figure 6 Plates dimensions and hole positions

Table 1 Normal holes diameters

	Bolt	Bolt diameter	Clearance	Hole diameter
Diameters for normal holes	M24	24mm	2mm	26mm
	M39	39mm	3mm	42mm

Strengths for M24 and M39 bolts, as per EN 1993-1-8 [43], are provided in Table 2, the values are based on the mentioned material properties: class 8.8 for bolts and class S355 for steel plates. Figure 7 displays the combined shear and tension interaction diagram.

Table 2 Calculated strengths for the proposed bolts

	$F_{t,Rd}$	$F_{v,Rd}$	$F_{b,Rd}$	$B_{p,Rd}$
M24	203.30 kN	135.60 kN	470.70 kN	573.20 kN
M39	562.20 kN	374.80 kN	764.40 kN	955.20 kN

where $F_{t,Rd}$ is the tensile resistance, $F_{v,Rd}$ is the shear resistance per shear plane, $F_{b,Rd}$ is the bearing resistance of the bolt, and $B_{p,Rd}$ the punching resistance.

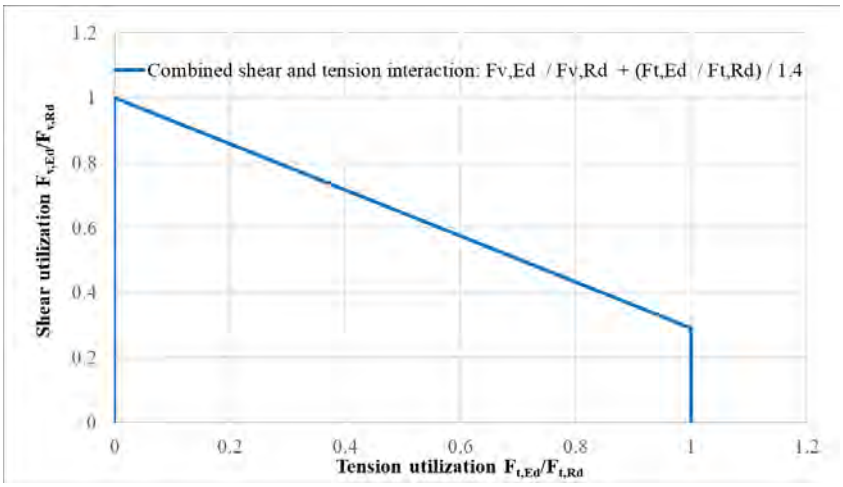

Figure 7 Combined shear and tension interaction

An analysis using the steel connection module of the Idea StatiCa software [45] was conducted to identify effective internal forces in the connection components by subjecting the connection to an increasing tension load up to 590 kN, which represents the failure load of the connection based on the Idea StatiCa results. This design check focused on the steel (bolts and plates) elements of the connection. Figures 8 and 9 display the strain and stress results for the steel plates in the connection. From these results, it is evident that the 590 kN load keeps the steel plates below the 5% value, considered the limit of plastic strain (ε_{lim}) [46]. The stress and strain distribution suggests that the plates can effectively transmit the applied tension load.

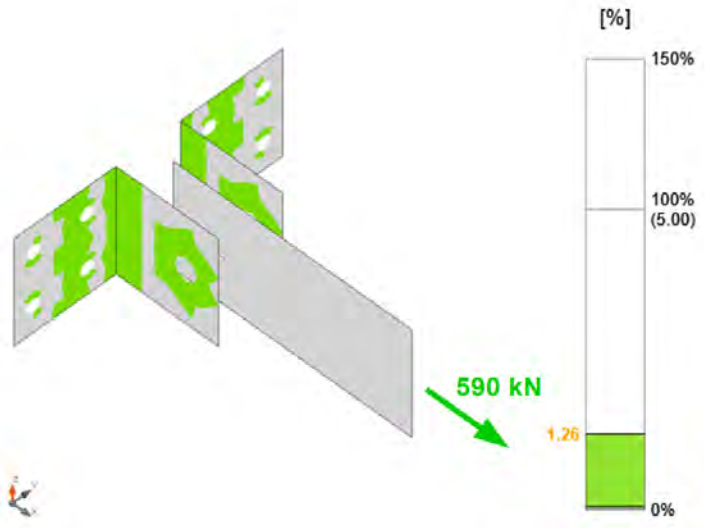

Figure 8 Steel plates strain check

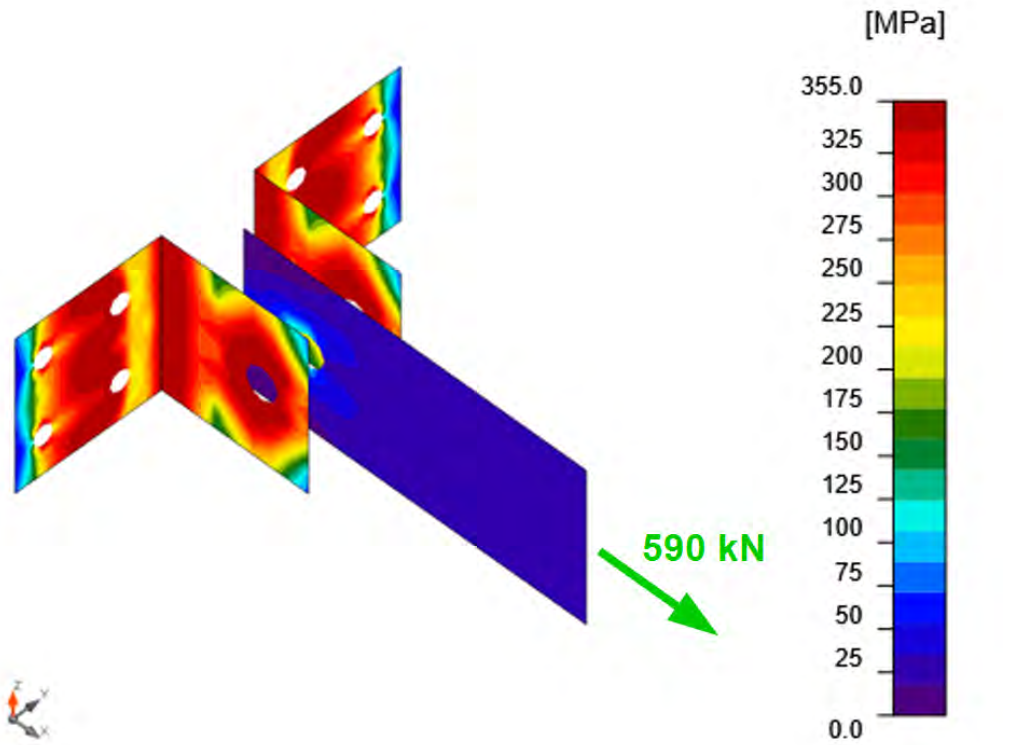

Figure 9 Steel plates equivalent stresses

The Idea StatiCa internal forces for the bolts used in this connection are shown in Table 3. Examining the combined shear and tension interaction results reveals that the M39 bolt, serving as the beam web connector (Figure 10), approaches the combined load limit with a value of 0.97. The calculation also indicates that the two M24 bolts nearest to the beam web, M24-1 and M24-2, as shown in Figure 10, have the highest contribution out of the four column fork connectors, 0.84 compared to 0.41. Considering a 25 mm diameter embedded bar in the column fork and the design yield limit for S500 steel (435 N/mm2), the tension capacity for one bar is 231.42 kN. Given the previous results, these embedded bars can withstand the tension forces transmitted from the associated M24 bolts.

Table 3 Calculated forces for all the M24 bolts

	$F_{t,Ed}$	$F_{v,Ed}$	$F_{t,Rd}$	$F_{v,Rd}$	$F_{v,Ed} / F_{v,Rd} + (F_{t,Ed} / F_{t,Rd}) / 1.4 \leq 1.0$
M24 – 1	164.20 kN	35.70 kN	203.30 kN	135.60 kN	0.84 < 1.00
M24 – 2	164.20 kN	35.70 kN	203.30 kN	135.60 kN	0.84 < 1.00
M24 – 3	46.70 kN	33.20 kN	203.30 kN	135.60 kN	0.41 < 1.00
M24 – 4	46.70 kN	33.20 kN	203.30 kN	135.60 kN	0.41 < 1.00
M39	141.50 kN	295.00 kN	562.20 kN	374.80 kN	0.97 < 1.00

where $F_{t,Ed}$ is the applied tensile load, and $F_{v,Ed}$ is the is the applied shear load.

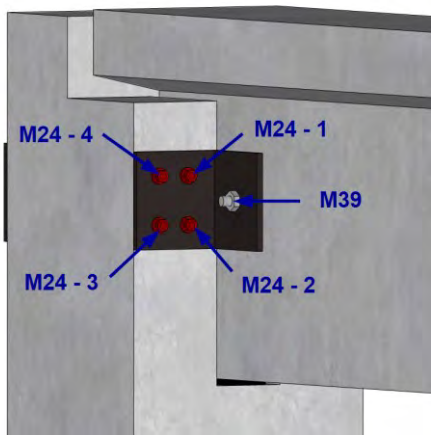

Figure 10 Bolt names for the tension and shear results

Based on the calculations, the load capacity of the connection appears to be governed by the strength capacity of the M39 beam web connector. With the current proposed configuration, the connection capacity is estimated at 590 kN. The strength capacity of the proposed connection (Figure 2) is nearly three times greater than the dowel connection solution which had a capacity of approximately 200kN [39, 40].

It is also essential to assess the strength of the column fork and determine if it can withstand the loads transferred from the beam via the connection. The fork section was examined as depicted in Figure 11, with the cross-section check performed according to EC2 [47] clause 6.5 for thick cantilever beams (Figure 12), using parameters from the Romanian EC2 National Annex [48]. The applied load on one side of the fork was 295 kN, half of the maximum capacity of the connection, 590 kN. Eurocode 2 Worked Examples [49] were used as a guide, specifically Example 6.10 for thick cantilever beams and Example 6.4 for determining the shear capacity of a given cross-section. The applied load was considered at a height of 450 mm relative to the base of the column (Figure 11), where the beam sits. Calculations demonstrated that the compressive stresses (σ=2.71 N/mm2) in node 1 (Figure 12) are lower than the maximum compressive stress applicable to the concrete node ($\sigma_{1Rd.max}$=12.04 N/mm2) as given by EC2 clause 6.5 [47]. The final check involved shear forces at the base of the column fork, where 8mm diameter stirrups at a 100mm pace provide a shear capacity of 842 kN, exceeding the applied load of 295 kN. Considering the column fork checks, the column capacity is sufficient to withstand the forces transmitted by the proposed connection without damaging the connection area.

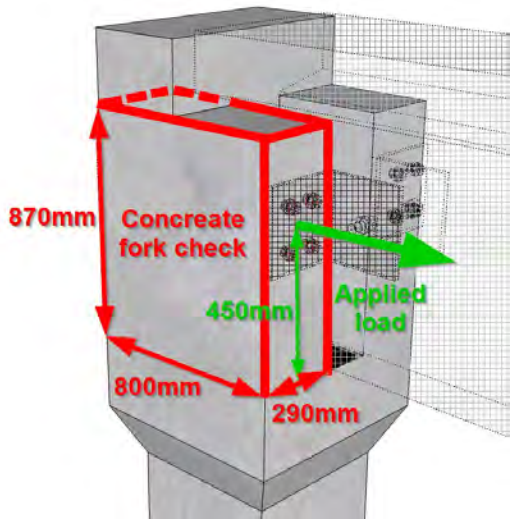

Figure 11 Column fork section to be checked

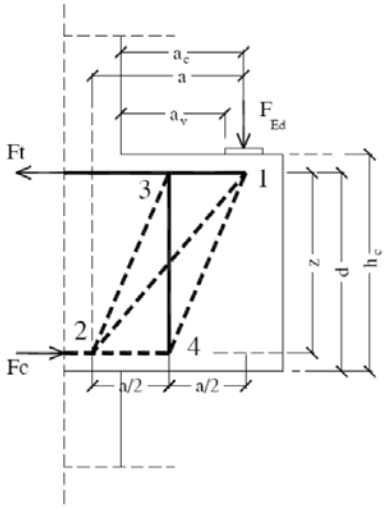

Figure 12 Thick cantilever beam strut and tie model [49]

4. Finite element model

To validate the initial empirical design check and compare the behaviour of the proposed connection with the dowel connection, a finite element model that replaces the dowel connection with the new proposed solution is required. To obtain comparable results, it is necessary to use the DIANA FEA [50] calibrated models developed in previous work [40].

The concrete components, namely the beam and column, were modelled with isoparametric solid brick CHX60 finite elements [50]. The software automatically picks reinforcement elements based on the concrete volume element type. For CHX60 concrete elements, truss reinforcements use CL9TR [50] elements, which handle only axial strains and stresses, while dowel-like beam reinforcements that also resist shear forces use CL18B [50] elements. For plane interfaces, quadrilateral interface element type CQ48I [50] was employed, commonly used for surface-to-surface contact and boundary interfaces, with normal and shear stiffness values assigned. The steel plates were modelled as CHX60 solid elements, while the bolts and embedded bars were modelled as line elements, namely CL18B, the same as for the dowel elements in the previous connections. Due to the relatively small size of the connection elements compared to the entire model, some simplifications were needed when modelling the connection geometry. As a result, the embedded column bars and bolts were considered continuous and had the same material properties for the entire element. CQ48I plane interface elements were used to model the interface between steel plates and concrete parts. The geometry of the model was built based on the shop drawings used in the experiments and built to full scale (Figure 13).

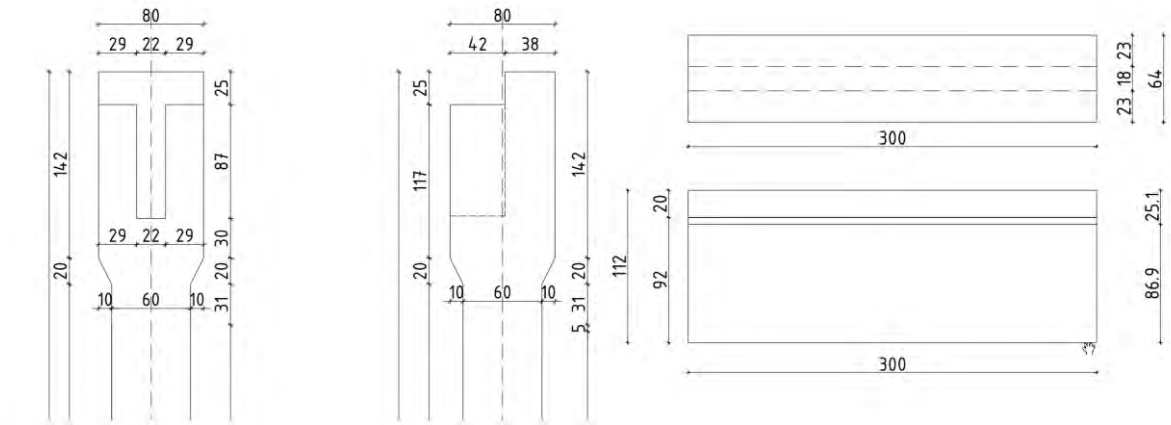

Figure 13 Element dimensions

Material constitutive models for the numerical simulations were chosen in light of the deformations

observed in the experimental tests. To accurately capture the plastic behaviour of the materials in critical areas, nonlinear constitutive models were implemented. The concrete elements used the "Maekawa-Fukuura Concrete Model" from the DIANA FEA material library, chosen for its capacity to capture material plasticization in critical regions and its good performance in quasi-static and hysteretic analysis. This model, an extension of a smeared cracking model, is based on Maekawa's research [51] and uses cyclic loading data. The implementation of the model was defined according to the software documentation [50, 52], and was combined with the model proposed by Vecchio and Collins [53] to account for the impact of lateral cracking that reduces the compressive strength of the concrete for large tensile strains perpendicular to the principal compressive direction. Concrete parameters are shown in Table 4.

Table 4 Maekawa-Fukuura Concrete model parameters

Linear properties	Mass density	2.5e-09 t/mm^3
	Strain at compressive strength	0.002
Tensile behaviour	Tensile strength	4.1 N/mm^2
	Plateau end strain	0.0002
	Power C	0.4
	Threshold angle	22.5°
Compressive Behaviour	Uniaxial compressive strength	68 N/mm^2
Reduction model	Vecchio and Collins 1993	0.6

The behaviour of all longitudinal reinforcements and stirrups was modelled using the Menegotto-Pinto plasticity model [54]. Reinforcement parameters were determined based on the S500 steel class used in the experiment, with specific parameters set according to the technical documentation of the software. The values used in this FE model are presented in Table 5.

Table 5 Menegotto-Pinto steel reinforcement parameters

Menegotto-Pinto steel reinforcement parameters	Young's modulus	194600 N/mm^2
	Poisson's ratio	0.3
	Mass density	7.85e-09 T/mm^3
	Yield stress	432.63N/mm^2
	Initial tangent slope	0.00286359
	Initial curvature parameter	20
	Constant a_1	18.5
	Constant a_2	0.15
	Constant a_3	0.01
	Constant a_4	7

The material properties of both steel plates and bolts were modelled using the Von Mises and Tresca plasticity model, with each yield limit of the element defined according to the material class and corresponding properties from the design codes, EN 1993-1-1 [42] for steel plates and EN 1993-1-8 [43] for fastening bolts.

The FE model was developed using quadratic elements. The size of the FE mesh was determined

based on the model size and the need for precise results within a reasonable computational time. The mesh was generated using the division meshing algorithm of the software, dividing edges into a specific number of elements to ensure uniform size across all mesh elements. The FE model geometry and material definition were similar with the ones used for modelling dowel connection (Figure 14) [40]. The dowel connection used one 32mm dowel bar on each side of the fork having a 20mm concrete coverage in the direction of the applied load. The mesh element sizes for the proposed connection varied between 50mm and 100mm (Figure 15), with finer mesh used in the column fork where damage was observed during experimental tests [39].

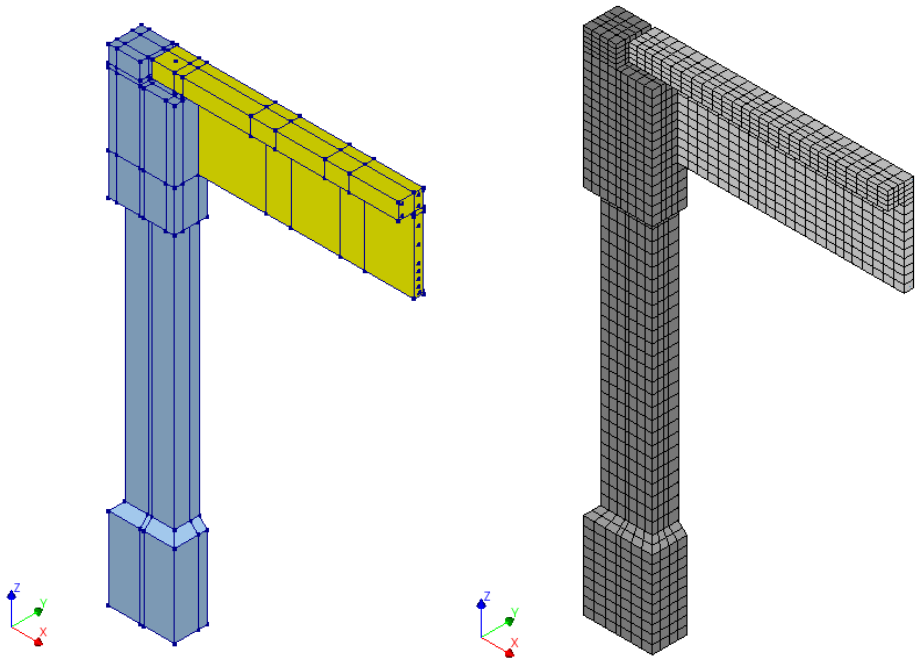

Figure 14 Dowel connection FE model

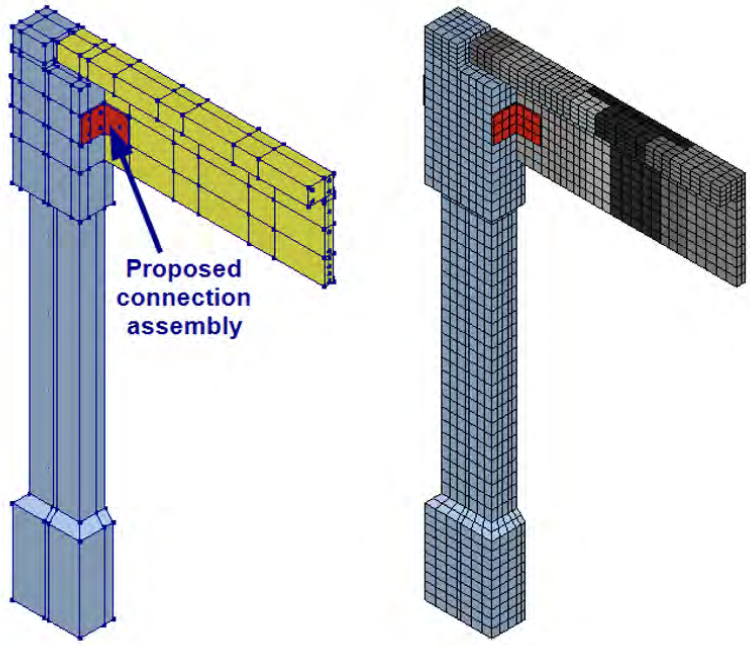

Figure 15 FE model geometry and meshing

The load was applied in the form of a point displacement at the end of the beam. A tie was created between the selected point and the face of the beam to ensure equal displacements in the X direction. This tie simulated the effect of the thick steel plate present at the end of the beam during

experimental tests, distributing the load uniformly. The obtained results will indicate the influence of the connection on the assembly and can be directly compared in terms of effects, maximum force, and failure force with the dowel connection benchmark model.
Two FE models were built with differences in the position of the connection assembly (Figure 16) to determine if there is any significant influence in the behaviour of the connection. For position 2 the entire connection was shifted upward by 100 mm. The proposed connection could not be positioned any lower because the beam connecter would pass through the pretensioned area of the beam web. These two positions represent the upper and lower bound limits for installing the proposed connection.

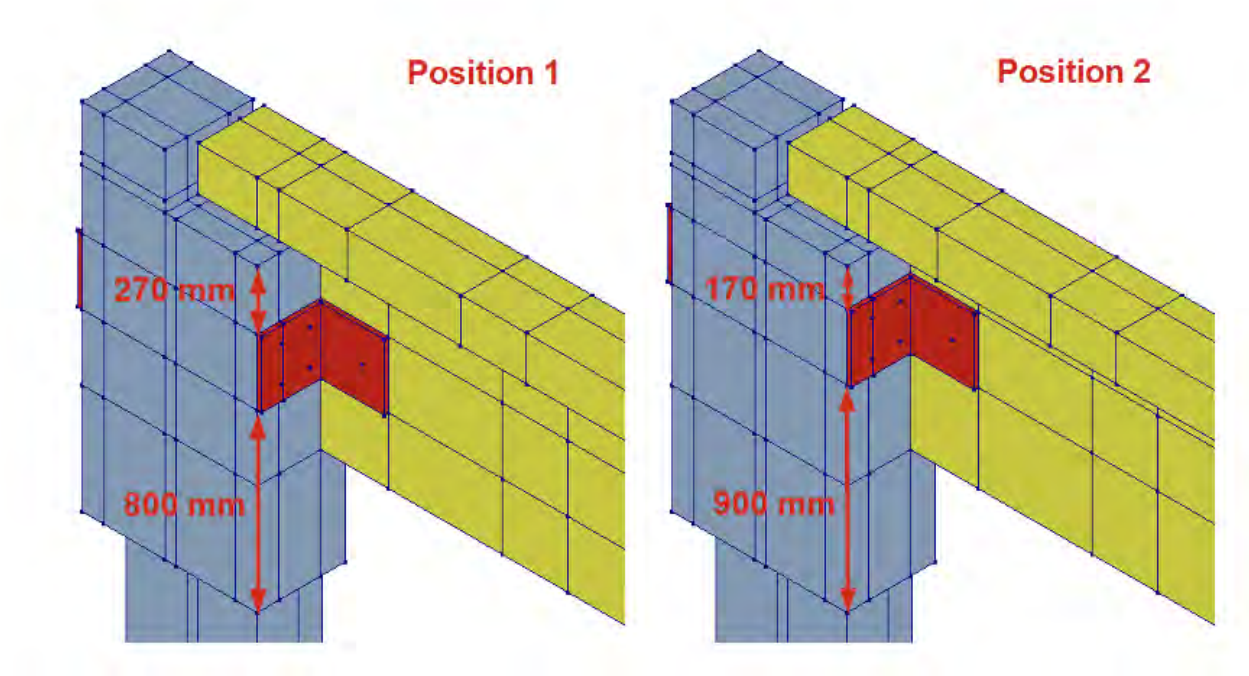

Figure 16 Connection position variation

4.1 Finite element analysis results

Figure 17 shows the force-displacement outcomes for the suggested connection in contrast with the benchmark dowel connection. The data indicates a considerable rise in failure load when using the proposed connection. The failure load peaks at around 450 kN for the first position of the connection, which is over double the load of the dowel connection. However, the location of the connection does not appear to greatly influence the failure load of the assembly. In this situation, the failure of the assembly is not driven by the failure of the connection but by the yielding of the longitudinal reinforcements in the column, as shown in Figures 18 and 19. The force is passed to the column via the connection, and a higher point of force application (Position 2) creates a larger bending moment at the base of the column. With no other significant damage around the connection and the beam, the maximum failure load is reduced due to the increased bending moment at the column base.

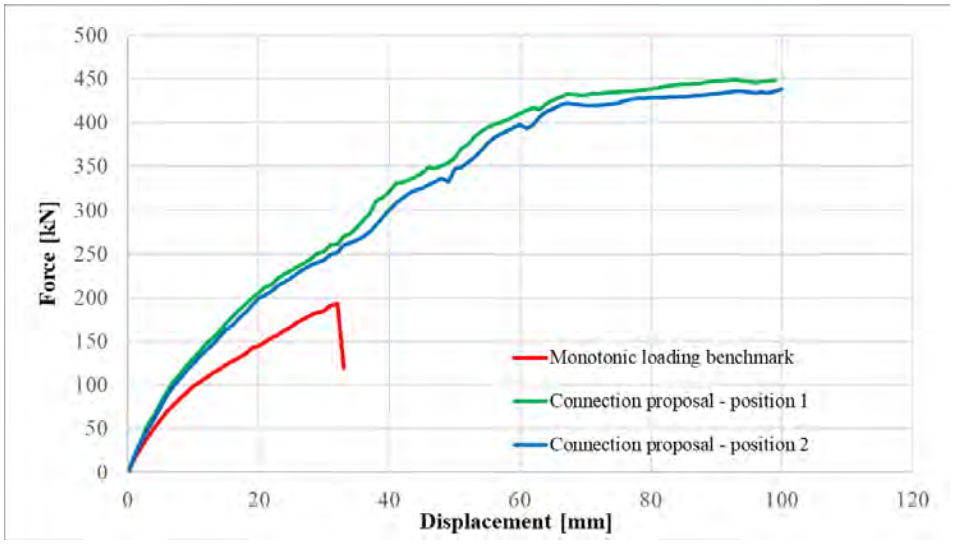

Figure 17 Force-displacement diagrams comparison between dowel connection (benchmark) and the proposed connection

Figure 18 shows the stress distribution within the longitudinal reinforcements of the column, corresponding to the configuration of the connection at Position 1, when yielding starts, at a displacement load of 50 mm, and at the end of the analysis, at approximately 100 mm displacement load. The figure shows that only the reinforcements at the rear of the column begin to yield in the first stage. As the displacement load increases, the other reinforcements start yielding until the analysis ends, indicating column failure. The forces within the longitudinal reinforcements of the column are considerably greater than those observed in the prior analysis of any dowel connection models. By comparing the force-displacement result for the entire assembly, as displayed in Figure 17, with the stress distribution within the longitudinal reinforcements from Figure 18, it can be deduced that there are no significant increases in the equivalent loading force between the 60 mm displacement and the final 100 mm displacement. This is because the column is getting close to its maximum capacity.

Figure 19 displays the stress distribution in the longitudinal reinforcement of the column for the model with the connection configuration corresponding to Position 2. The results align closely with those seen for Position 1 in Figure 18, and similar conclusions can be made. The position of the connection does not notably influence the stress distribution in the longitudinal reinforcements. However, in both scenarios, it results in stresses surpassing the yielding limit. As mentioned earlier, these findings suggest a strong association between the peak loading force and the column failure due to the yielding of the longitudinal reinforcements. Nonetheless, it is essential to study the behavior of the connection itself and the adjacent concrete areas to validate the assumption related to the column failure.

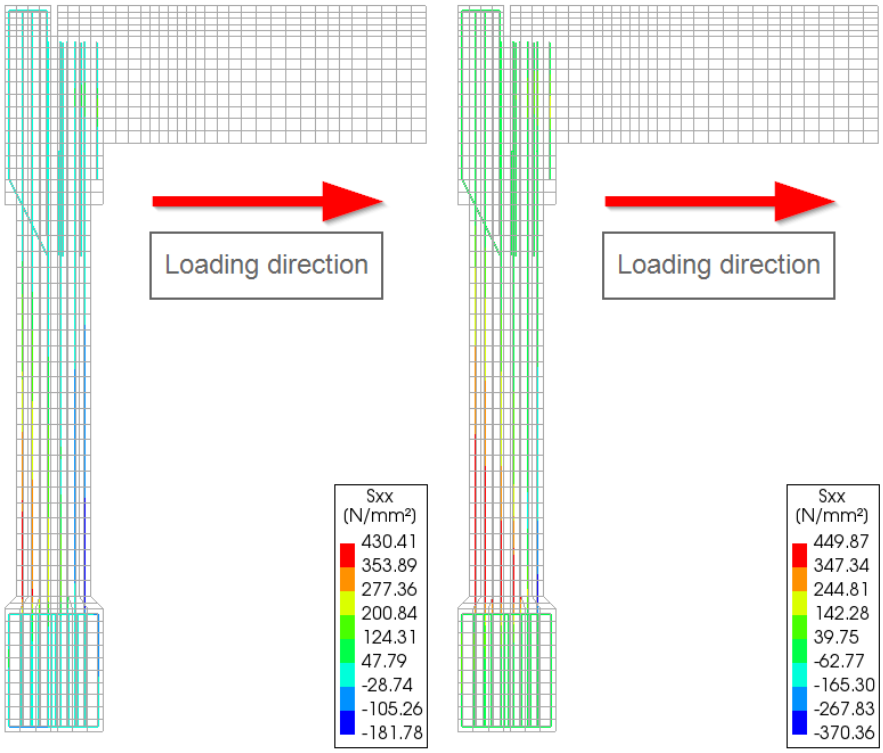

Figure 18 Maximum longitudinal reinforcement stresses for Position 1, at the start of yielding - 50mm displacement (left), and the end of the analysis - 100 mm displacement (right)

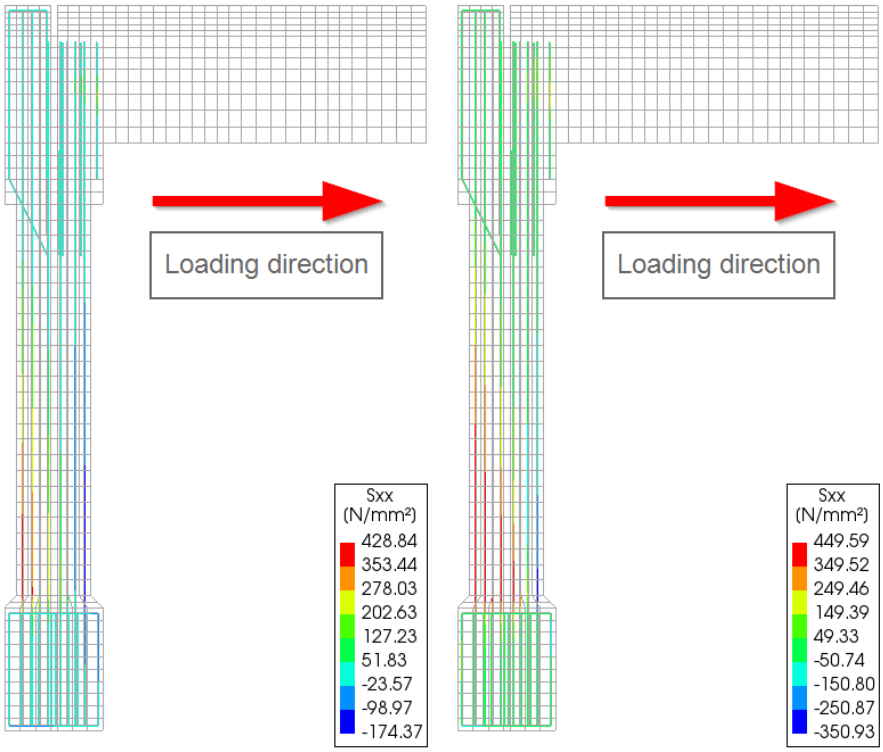

Figure 19 Maximum longitudinal reinforcement stresses for Position 2, at the start of yielding - 50mm displacement (left), and the end of the analysis - 100 mm displacement (right)

Figures 20 and 21 illustrate the stress change in all the bolts of the column in relation to the displacement loading of the assembly, for Position 1 and Position 2 of the connection, respectively. The results reveal that the maximum stresses in the M24-1 bolt exceed the yielding limit. However, the M24-1, M24-3, and M24-4 bolts remain within the elastic range, suggesting that at the end of

the analysis, the connection retains sufficient capacity. The bolt positions are shown in Figure 10. The DIANA FEA models account for the deformed shape of the column, resulting in a d stress distribution in the two bolts closest to the beam web, as this causes eccentric loading of the connection. Conversely, in the results from the simple calculations using Idea StatiCa, where only the connection was analysed, the load was aligned with the connection, leading to an even distribution of forces in the M24-1 and M24-2 bolts, as well as the M24-3 and M24-4 bolts, which are in the second row of the connection. Both outcomes, from DIANA FEA and Idea StatiCa, affirm that the highest loads are located in the first row of the connection (M24-1 and M24-2). However, considering the eccentric loading, additional bolts are necessary to provide redundancy to the connection. The M39 bolt of the beam web connector is loaded below the yielding limit, suggesting that this arrangement offers adequate strength to transfer the horizontal loads from the beam to the column. In terms of capacity, the overall behavior of the connection is considerably superior to that of the dowel connection solution.

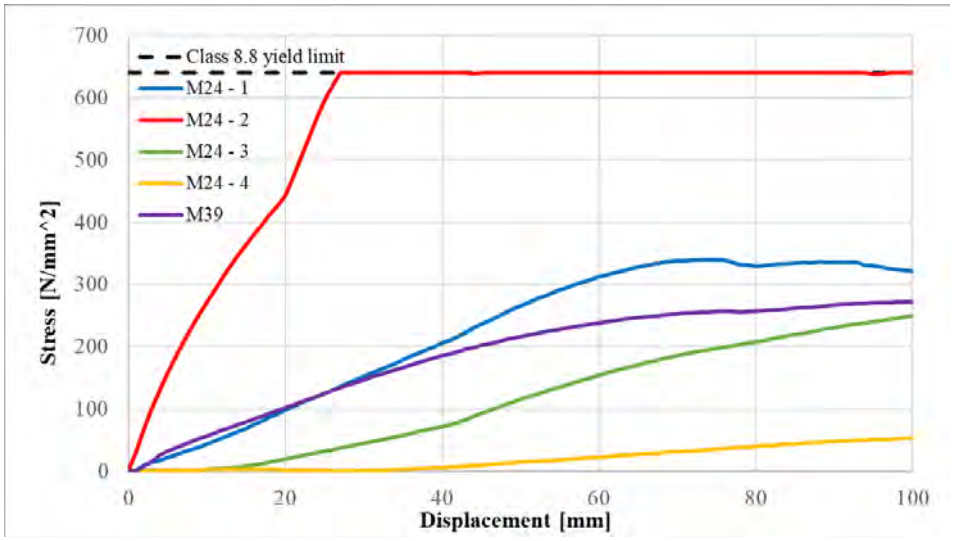

Figure 20 Maximum Von Mises stresses variation in the M24 and M39 elements for Position 1 of the connection

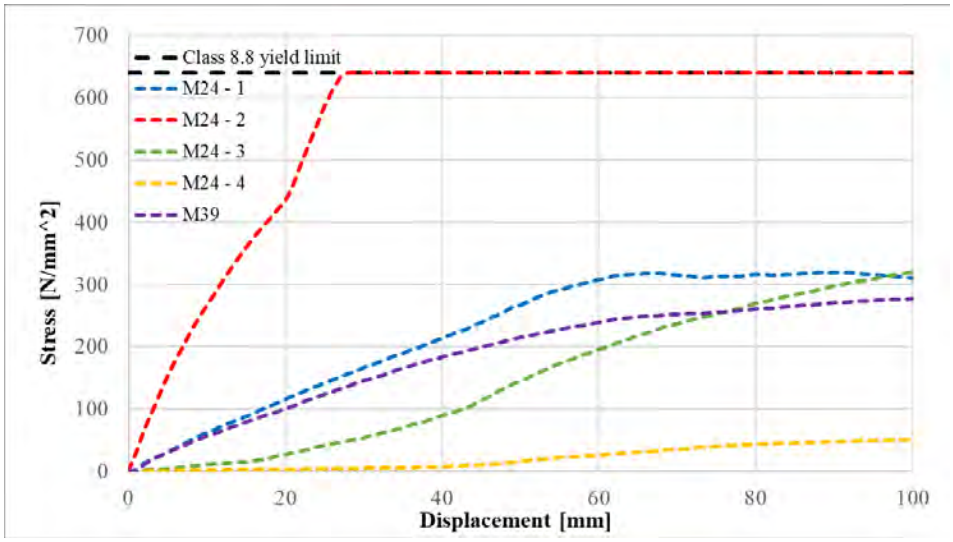

Figure 21 Maximum Von Mises stresses variation in the M24 and M39 elements for Position 2 of the connection

As mentioned earlier, the yielding of the longitudinal reinforcements of the column increased progressively across all reinforcement rows until the analysis ended, indicating the base of the column was undergoing plasticisation. This process is the anticipated dissipative mechanism for inversed pendulum structures. Figure 22 presents the row numbering for the longitudinal columns.

Figures 23 and 24 provide a detailed view of stress variation in the longitudinal reinforcements in relation to the applied displacement, for Position 1 and Position 2 of the connection, respectively. Both scenarios present similar stress variations across all the longitudinal reinforcement rows up to the analysis termination.
Comparing the stress variation, in the bolts of the connection and the longitudinal reinforcements of the column, supports the theory that the base of the column initiates the dissipative plasticisation process through the yielding of the longitudinal reinforcements, while the proposed beam-to-column connection still has additional loading capacity. The configuration of the connection ensures redundancy in transmitting the horizontal load, even if bolt M24-2 is reaching its design capacity, via the remaining three bolts.

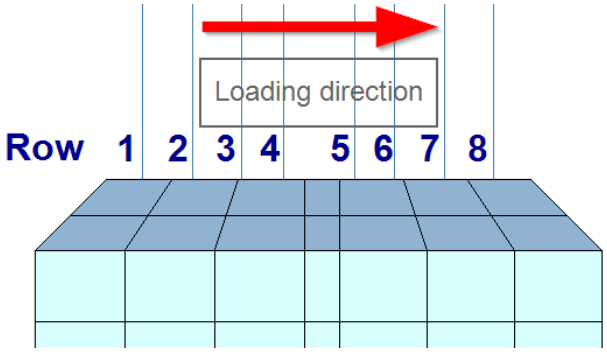

Figure 22 Column longitudinal reinforcement rows

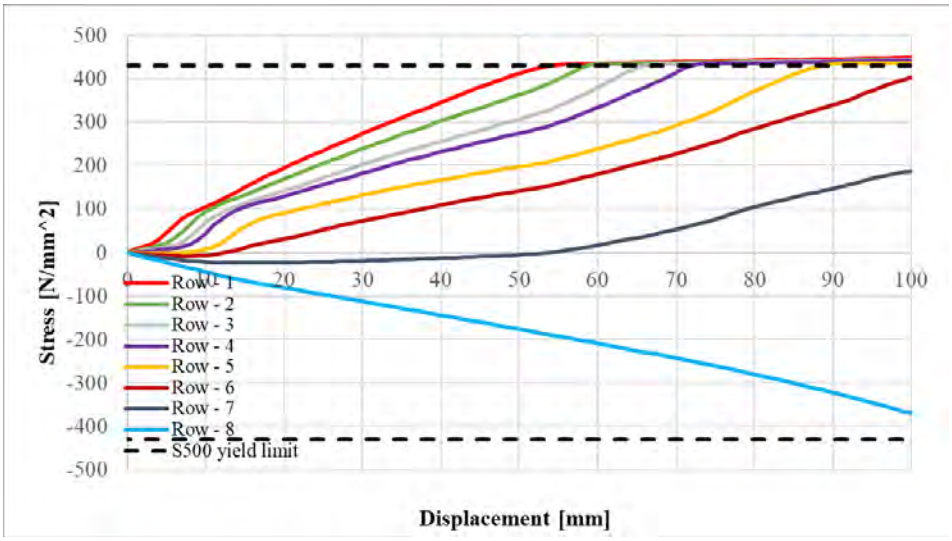

Figure 23 Maximum stresses variation for each longitudinal reinforcement row in the column for Position 1 of the connection

The findings regarding stress variation in the longitudinal reinforcement, as illustrated in Figures 23 and 24, indicate that rows 1 through 5 reach the yielding limit at the end of the analysis, and only the reinforcements in row 8 exhibit compressive stresses. The results from previous study [40] concerning the longitudinal reinforcement of the column reveal that when using the dowel connection, the stresses in the longitudinal reinforcements were significantly smaller, peaking at approximately 200kN. Furthermore, in those cases the connection (dowel) failed before these stresses could reach the yield limit.

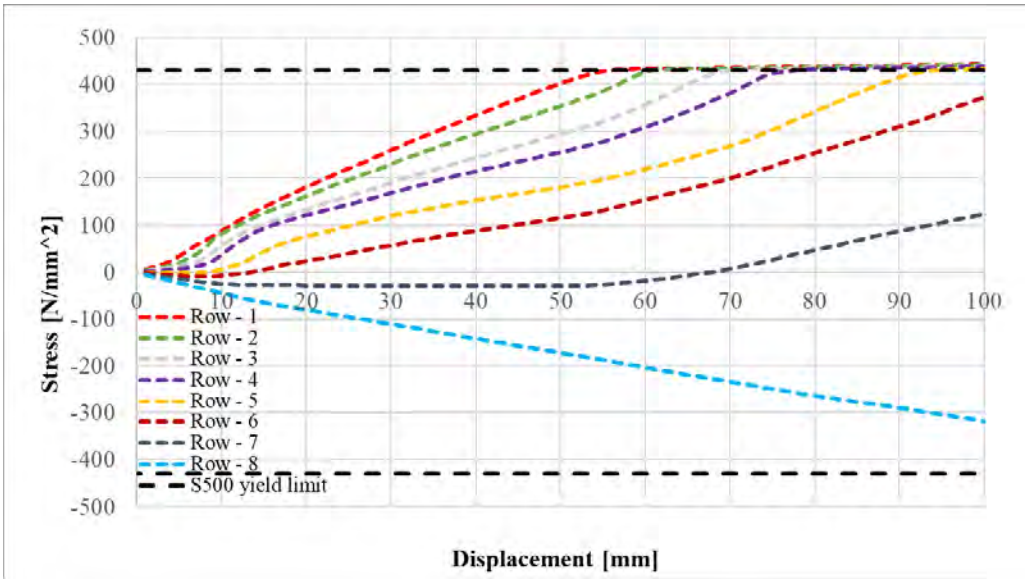

Figure 24 Maximum stresses variation for each longitudinal reinforcement row in the column for Position 2 of the connection

The crack pattern plots and the regular crack strain values, as depicted in Figure 25 for both connection positions, show a high concentration of crack strains at the column base and surrounding the connection area. For the proposed connection, the highest normal crack strain values (E_{knn}) occur at the column base, which also has the largest stresses in the longitudinal reinforcements. The E_{knn} values suggest that the cracks at the column base and around the connection have reached a stabilized stage (E_{knn}>0.008), based on the normal crack strain values and the limits for the different cracking stages [55]. The crack strains in the beam primarily result from the tensions introduced by the beam web connector (M39).

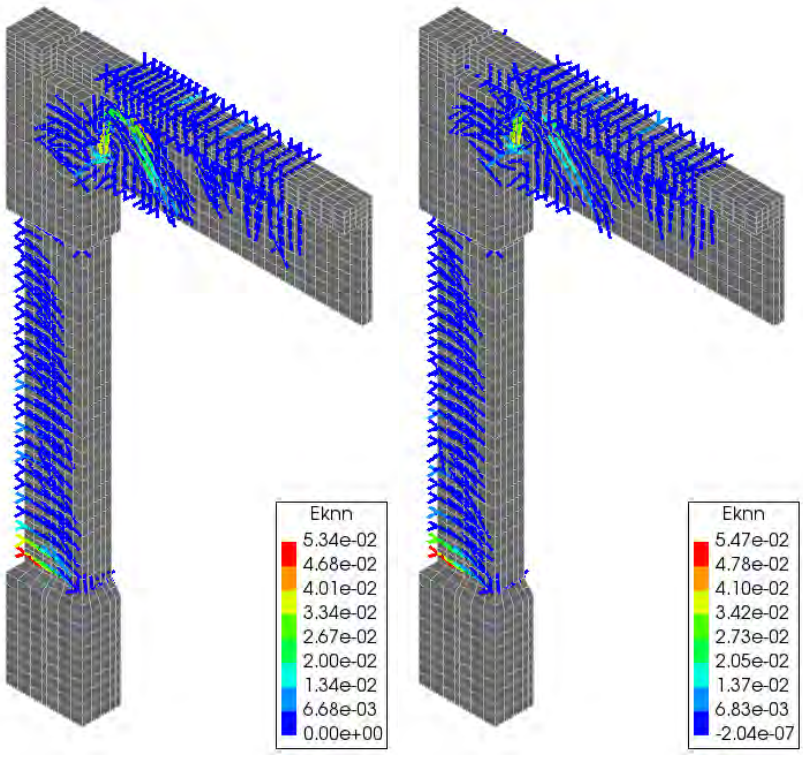

Figure 25 Crack pattern plots and normal crack strains values at the end of the analysis for Position 1 (left) and Position 2 (right)

5. Conclusions

- The primary focus of this section of the research was to assess whether the proposed connection could offer a greater capacity compared to the dowel connection. Consequently, only a restricted selection of parameters and geometries was employed for the investigations.
- The research concludes that the proposed connection significantly enhances the strength capacity compared to the dowel connection solution, with the maximum equivalent load more than doubling from 200 kN to 450 kN.
- This increased capacity results in higher loads being transferred to the column, initiating the dissipative mechanism via plasticisation of the column base.
- In earlier cases, the stresses in the longitudinal reinforcements were considerably lower, and the connection could not bear higher loads.
- Modifications to the dowel connection would result in the same outcome, as not only is the dowel itself a critical point, but the outcome is also influenced by the minimal concrete coverages, which cannot be increased in this configuration.
- The proposed connection overcomes the geometric peculiarities of the precast elements and provides enough horizontal capacity to determine the failure of the column, which is the key dissipative mechanism for inversed pendulum structures.
- The configuration of the connection also offers opportunities for further improvement, as each component can be individually tailored to achieve maximum efficiency.

Acknowledgements

The financial support by CONSOLIS is greatly acknowledged.
The research activities were supported by the project POCU/380/6/13/123927 – ANTREDOC, "Entrepreneurial competencies and excellence research in doctoral and postdoctoral studies programs", project co-funded from the European Social Fund through the Human Capital Operational Program 2014-2020.

6. References

[1] European Comision, "Design Guidelines for Connections of Precast Structures under Seismic Actions," Joint Research Centre of the European Commission, Luxembourg, 2012.

[2] G. Magliulo, M. Ercolino, M. Cimmino, V. Capozzi and G. Manfredi, "FEM analysis of the strength of RC beam-to-column dowel connections under monotonic actions," *Construction and Building Materials,* vol. 69, pp. 271-284, 2014.

[3] G. Magliulo, D. Bellotti, M. Cimmino and R. Nascimbene, "Modeling and Seismic Response Analysis of RC Precast Italian Code-Conforming Buildings," *JOURNAL OF EARTHQUAKE ENGINEERING,* vol. 22, pp. 140-167, 2018.

[4] L. Liberatore, L. Sorrentino, D. Liberatore and L. D. Decanini, "Failure of industrial structures induced by the Emilia (Italy) 2012 earthquakes," *Engineering Failure Analysis,* vol. 34, pp. 629-647, 2013.

[5] M. Ercolino, G. Magliulo and G. Manfredi, "Failure of a precast RC building due to Emilia-Romagna earthquakes," *Failure of a precast RC building due to Emilia-Romagna earthquakes,* vol. 118, pp. 262-273, 2016.

[6] E. Artioli, R. Battaglia and A. Tralli, "Effects of May 2012 Emilia earthquake on industrial

buildings of early ’900 on the Po river line," *Engineering Structures,* vol. 56, pp. 1220-1233, 2013.

[7] M. Saatcioglu, D. Mitchell, R. Tinawi, N. J. Gardner, A. G. Gillies, A. Ghobarah, D. L. Anderson and D. Lau, "The August 17, 1999, Kocaeli (Turkey) earthquake — damage to structures," *Can. J. Civ. Eng. ,* vol. 28, pp. 715-737, 2001.

[8] B. Faggiano, B. Iervolino, G. Magliulo, G. Manfredi and I. Vanzi, "Post-event analysis of industrial structures behavior during L’Aquila earthquake," in *Progettazione Seismica*, 2009, pp. 203-208.

[9] G. Toniolo and A. Colombo, "Precast concrete structures: the lessons learned from the L’Aquila earthquake," *Structural Concrete,* vol. 13, no. 2, pp. 73-86, 2012.

[10] G. Magliulo, M. Ercolino, C. Petrone, O. Coppola and G. Manfredia, "The Emilia Earthquake: Seismic Performance of Precast Reinforced Concrete Buildings," *Earthquake Spectra,* vol. 30, no. 2, pp. 891-912, 2014.

[11] D. A. Bournas, P. Negro and F. F. Taucer, "Performance of industrial buildings during the Emilia earthquakes in Northern Italy and recommendations for their strengthening," *Bulletin of Earthquake Engineering,* vol. 12, pp. 2383-2404, 2014.

[12] F. Cornali, A. Belleri, A. Marini and P. Riva, "Influence of modelling assumptions in the expected loss evaluation of a precast industrial building," in *EURODYN 2017*, Rome, 2017.

[13] C. Demartino and G. Monti, "Low-LOD code-driven identification of the high seismic risk areas for industrial buildings in Italy," *Bulletin of Earthquake Engineering,* vol. 18, p. 4421–4452, 2020.

[14] N. Buratti, F. Minghini, E. Ongaretto, M. Savoia and N. Tullini, "Empirical seismic fragility for the precast RC industrial buildings damaged by the 2012 Emilia (Italy) earthquakes," *Earthquake Engng Struct. Dyn.,* vol. 46, no. 14, pp. 2317-2335, 2017.

[15] N. BATALHA, H. RODRIGUES and H. VARUM, "Seismic performance of RC precast industrial buildings—learning with the past earthquakes," *Innovative Infrastructure Solutions,* vol. 4, 2019.

[16] A. BELLERI, E. BRUNESI, R. NASCIMBENE, M. PAGANI and P. RIVA, "Seismic Performance of Precast Industrial Facilities Following Major Earthquakes in the Italian Territory," *Journal of Performance of Constructed Facilities,* vol. 29, no. 5, 2015.

[17] C. Casotto, V. Silva, H. Crowley, R. Nascimbene and R. Pinho, "Seismic fragility of Italian RC precast industrial structures," *Engineering Structures,* vol. 94, pp. 122-136, 2015.

[18] A. V. Pollini, N. Buratti and C. Mazzotti, "Behavior factor of concrete portal frames with dissipative devices based on carbon-wrapped steel tubes," *Bulletin of Earthquake Engineering ,* vol. 19, p. 553–578, 2021.

[19] A. Titi, F. Biondini and G. Toniolo, "Seismic assessment of existing precast structures with dry-friction beam-to-column joints," *Bull Earthquake Eng,* vol. 16, p. 2067–2086, 2018.

[20] R. Sousa, N. Batalha, V. Silva and H. Rodrigues, "Seismic fragility functions for Portuguese RC precast buildings," *Bulletin of Earthquake Engineering,* vol. 19, p. 6573–6590, 2021.

[21] CEN (Comité Européen de Normalisation), "Eurocode 8: Design of structures for earthquake resistance – Part 1: General rules, seismic actions and rules for buildings (EN 1998-1)," CEN, Brussels, 2004.

[22] C. Demartino, I. Vanzi, G. Monti and C. Sulpizio, "Precast industrial buildings in Southern Europe: loss of support at frictional beam-to-column connections under seismic actions," *Bull Earthquake Eng,* vol. 16, p. 259–294, 2018.

[23] P. Carydis, I. Psycharis and H. Mouzakis, "PRECAST EC8: seismic behaviour of precast concrete structures with respect to Eurocode 8. Final Report of the contribution of LEE/NTUA.," FP5 Project No G6RD-CT-2002-00857, 2007.

[24] G. Magliulo, V. Capozzia, G. Fabbrocino and G. Manfredi, "Neoprene–concrete friction relationships for seismic assessment of existing precast buildings," *Engineering Structures,* vol. 33, pp. 532-538, 2011.

[25] C. Demartino, G. Monti and I. Vanzi, "Seismic loss-of-support conditions of frictional beam-to-column connections," *Structural Engineering and Mechanics,* vol. 61, no. 4, pp. 527-538, 2017.

[26] M. Fischinger, B. Zoubek, M. Kramar and T. Isaković, "Cyclic Response of Dowel Connections in Precast Structures," in *15 WCEE*, Lisboa, 2012.

[27] M. Kramar, T. Isaković and M. Fischinger, "Seismic collapse risk of precast industrial buildings with strong connections," *Earthquake Engineering & Structural Dynamics,* vol. 39, no. 8, pp. 847-868, 2009.

[28] M. Cimmino, G. Magliulo and G. Manfredi, "Seismic collapse assessment of new European single-story RC precast buildings with weak connections," *Bulletin of Earthquake Engineering,* vol. 18, p. pages6661–6686, 2020.

[29] J. Esmaeili and N. Ahooghalandary, "Introducing an easy-install precast concrete beam-to-column connection strengthened by steel box and peripheral plates," *Engineering Structures,* vol. 205, 2020.

[30] M. Senturk, S. Pul, A. Ilki and I. Hajirasouliha, "Development of a monolithic-like precast beam-column moment connection: Experimental and analytical investigation," *Engineering Structures,* vol. 205, 2020.

[31] "Experimental investigation of dry mechanical beam–column joints for precast concrete based frames," *The Structural Design of Tall and Special Buildings,* vol. 26, no. 1, 2017.

[32] M. Rajeswari and K. Jaya, "Cyclic performance of emulative precast beam to column connection with corbel using dowel bar," *Revista de la Construcción,* vol. 21, no. 2, pp. 354-367, 2022.

[33] D. Guan, C. Jiang, Z. Guo and H. Ge, "Development and Seismic Behavior of Precast Concrete Beam-to-Column Connections," *Journal of Earthquake Engineering,* vol. 22, no. 2, pp. 234-256, 2018.

[34] R. Ketiyot and C. Hansapinyo2, "Seismic performance of interior precast concrete beam-column connections with T-section steel inserts under cyclic loading," *EARTHQUAKE ENGINEERING AND ENGINEERING VIBRATION ,* vol. 17, pp. 355-369, 2018.

[35] S. Bahrami, M. Madhkhan, F. Shirmohammadi and N. Nazemi, "Behavior of two new moment resisting precast beam to column connections subjected to lateral loading," *Engineering Structures,* vol. 132, p. 808–821, 2017.

[36] R. Sousa, N. Batalha and H. Rodrigues, "REVIEW OF STRATEGIES FOR MODELLING BEAM-TO-COLUMN CONNECTIONS IN EXISTING PRECAST INDUSTRIAL RC BUILDINGS," in *Congresso de Métodos Numéricos em Engenharia*, Guimarães, Portugal, 2019.

[37] W. Huang, G. Hu, X. Miao and Z. Fan, "Seismic performance analysis of a novel demountable precast concrete beam-column connection with multi-slit devices," *Journal of Building Engineering,* vol. 44, 2021.

[38] C. Tong, J. Wu and C. Li, "A novel precast concrete beam-to-column connection with replaceable energy-dissipation connector: Experimental investigation and theoretical analysis," *Bulletin of Earthquake Engineering ,* vol. 19, p. 4911–4943, 2021.

[39] M. G. Moldovan, M. Nedelcu and Z. Kovacs, "CYCLIC BEHAVIOUR OF BEAM-COLUMN DOWEL CONNECTION IN PRECAST ELEMENTS," in *4th World Congress in Computational Mechanics (WCCM)*, Virtual Congress, 2020.

[40] M. G. Moldovan and M. Nedelcu, "Finite element modelling of a beam to column dowel

connection calibrated on experimental data," *Acta Technica Napocensis: Civil Engineering & Architecture,* 2023.

[41] C. A. Apostolopoulos, M. P. Papadopoulos and S. G. Pantelakis, "Tensile behavior of corroded reinforcing steel bars BSt 500s," *Construction and Building Materials,* vol. 20, pp. 782-789, 2006.

[42] CEN (Comité Européen De Normalisation), "Eurocode 3: Design of steel structures - Part 1-1: General rules and rules for buildings," CEN, Brussels, 2005.

[43] CEN (Comité Européen De Normalisation), "Eurocode 3: Design of steel structures - Part 1-8: Design of joints," CEN , Brussels, 2009.

[44] CEN (Comité Européen De Normalisation), "EN 1090-2: Execution of steel structures and aluminium structures - Part 2: Technical requirements for steel structures," CEN, Brussels, 2011.

[45] IDEA RS s.r.o., "IDEA Connection 8 - User guide," IDEA StatiCa s.r.o., Brno.

[46] CEN (Comité Européen De Normalisation), "Eurocode 3 - Design of steel structures - Part 1-5: Plated structural elements," CEN, Brussels, 2006.

[47] CEN (Comité Européen de Normalisation), "Eurocode 2: Design of concrete structures - Part 1-1: General rules and rules for buildings," CEN, Brussels, 2004.

[48] Asociația de Standardizare din România (ASRO), "SR EN 1992-1-1/NB - Eurocode 2: Design of concrete structures - Part 1-1: General rules and rules for buildings. National Annex," ASRO, Bucharest, 2008.

[49] European Concrete Platform ASBL, "EUROCODE 2 WORKED EXAMPLES," European Concrete Platform ASBL, Brussels, 2008.

[50] DIANA FEA BV, *DIANA Finite Element Analysis - Documentation release 10.5,* Delft: DIANA FEA BV, 2021.

[51] N. Li, K. Maekawa and H. Okamura, "Contact density model for stress transfer across cracks in concrete," *J. of the Faculty of Engineering,* no. 1, pp. 9-52, 1989.

[52] K. Maekawa, H. Okamura and A. Pimanmas, Non-Linear Mechanics of Reinforced Concrete, New York: Spon Press, 2003.

[53] F. J. Vecchio and M. P. Collins, "Compression response of cracked reinforced concrete," *J. Struct. Eng.,* vol. 119, pp. 3590-3610, 1993.

[54] M. Menegotto and P. E. Pinto, "Method of analysis for cyclically loaded R.C. plane frames including changes in geometry and non-elastic behaviour of elements under combined normal force and bending," in *IABSE Symposium on Resistance and ultimate Deformability of Structures Acted on by Well-Defined Repeated Loads*, Lisbon, 1973.

[55] D. Schlicke, E. M. Dorfmann, E. Fehling and N. V. Tue, "Calculation of maximum crack width for practical design of reinforced concrete," *Civil Engineering Design,* vol. 3, pp. 45-61, 2021.